

Relaxation in filled polymers: A fractional calculus approach

Ralf Metzler

Department of Mathematical Physics, University of Ulm, Albert-Einstein-Allee 11,
D-89069 Ulm/Donau, Germany

Winfried Schick and Hanns-Georg Kilian

Department of Experimental Physics, University of Ulm, Albert-Einstein-Allee 11,
D-89069 Ulm/Donau, Germany

Theo F. Nonnenmacher

Department of Mathematical Physics, University of Ulm, Albert-Einstein-Allee 11,
D-89069 Ulm/Donau, Germany

(Received 8 June 1995; accepted 21 July 1995)

In recent years the fractional calculus approach to describing dynamic processes in disordered or complex systems such as relaxation or dielectric behavior in polymers or photo bleaching recovery in biologic membranes has proved to be an extraordinarily successful tool. In this paper we apply fractional relaxation to filled polymer networks and investigate the dependence of the decisive occurring parameters on the filler content. As a result, the dynamics of such complex systems may be well-described by our fractional model whereby the parameters agree with known phenomenological models. © 1995 American Institute of Physics.

I. INTRODUCTION

Relaxation processes deviating from the classical Debye- or exponential behavior include dielectric relaxation, stress relaxation, stress-strain relations, NMR relaxation or diffusion in materials like liquids, liquid crystals, polymer melts and solutions, amorphous polymers, rubbers or biopolymers. The deeper physical understanding of non-exponential relaxation processes belongs to the many unresolved problems in physics, as well as other topics occurring when one deals with such complex systems: the glass transition, the Vogel-Tamann-Fulcher (VTF) behavior for viscosity or the Williams-Landel-Ferry (WLF) relation for viscoelastic quantities or physical aging of polymers.^{1,2}

Non-exponential relaxation implies memory. A natural way to incorporate such memory effects is fractional calculus as shown by Glöckle and Nonnenmacher³⁻⁹ and Friedrich and Braun.¹⁰ Via the involved convolution integral the present state of the underlying system is influenced by all states at earlier times $t' = 0..t$. In recent papers³⁻⁹ the fractional relaxation concept with consideration of initial values was introduced and a physical interpretation of the parameters involved was given. Here, we first give a short summary of this concept before applying it to relaxation processes in filled polymers.

II. FRACTIONAL RELAXATION

We start off from the well-known standard solid or Zener model (see Fig. 1) with the constitutive equation

$$\sigma(t) + \tau_0 \frac{d\sigma(t)}{dt} = (G_m + G_e) \tau_0 \frac{d\epsilon(t)}{dt} + G_e \epsilon(t) \quad (1)$$

describing the stress-strain relationship. Here, the characteristic time constant $\tau_0 \equiv G_m / \eta_m$ was introduced (see Fig. 1).

This rather simple model exhibits a nonzero instant modulus, $G_m + G_e$, involves creep for intermediate times and shows solid behavior with the equilibrium modulus G_e for large times $t \ll \tau_0$. But for complex systems a more sophisticated approach is required. There, stress and strain are, in general, dependent on all strains and stresses at all times $t' \in (0, \dots, t)$, respectively, i.e. they are functionals of the form

$$\sigma(t) = \mathcal{S} [\epsilon(t)], \quad (2)$$

$$\epsilon(t) = \mathcal{E} [\sigma(t)]. \quad (3)$$

The functional dependence usually finds expression in a Boltzmann integral.¹¹ A special case of such an integral relation is given by involving a power law kernel (memory) leading to fractional derivatives. The background of such a kernel is discussed in Ref. 7. Thus a possible generalization of Eq. (1) can be acquired by the formal substitution of integer-order by fractional-order derivatives leading to

$$\begin{aligned} \sigma(t) - \sigma_0 + \tau_0^{-q} \frac{d^{-q} \sigma(t)}{dt^{-q}} \\ = G_e \tau_0^{-\mu} \frac{d^{-\mu} \epsilon(t)}{dt^{-\mu}} + (G_m + G_e) (\epsilon(t) - \epsilon_0) \end{aligned} \quad (4)$$

in the formulation as a fractional integral equation.³ ϵ_0 and σ_0 are the initial strain and stress, respectively. Here, the lhs of Eq. (1) was generalized by a fractional power q , the rhs involves μ , say. Two different fractional parameters are introduced as in general stress and strain *a priori* possess memories of different strengths. Both parameters fulfill the inequalities $0 \leq q, \mu \leq 1$, i.e. play an intermediate role in between Hooke's ($\sigma(t) = E\epsilon(t)$) and Trouton's ($\sigma(t) = \eta\dot{\epsilon}(t)$) laws.¹¹ q and μ must obey the additional restriction $q \geq \mu$ for sake of monotonically decreasing relax-

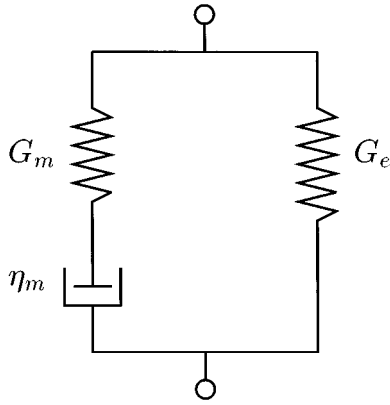


FIG. 1. Standard solid or Zener model.

ation functions.³ Whether such restrictions for the fractional parameters are readily implied via the Kramers–Kronig relations—which must be valid as the fractional model bases on a linear response theory—is topic of current investigations.

Schiessel and Blumen¹² and more recently Heymans and Bauwens¹³ use hierarchical model analogues of springs and dashpots to motivate fractional derivatives.

For $q = \mu$ one arrives at a fractional formulation of the Cole–Cole model whereas for $G_e = 0$ the fractional Maxwell model discussed by Nonnenmacher⁹ is recovered which reduces to the standard Maxwell model for $q \rightarrow 1$.

But there is one shortcoming issue. As our starting point, the standard Zener model, describes a solid system the fractional model should also display solid-like behavior. For the fractional integral Eq. (4) this does not hold true for $q > \mu$ but

it features a slow creep for larger times, an issue in direct consequence of the assignment of unequally strong memories (the strain has a “weaker” memory and thus relaxes faster than the strain causing a fluid-like behavior). To overcome this feature, the formal addition of a term $G_\infty \tau_0^{-q} d^{-q}/dt^{-q} \epsilon(t)$ involving a memory of strength q is necessary to balance the strain for large $t \gg \tau_0$. Thus one results in

$$\begin{aligned} \tau_0^{-q} \frac{d^{-q} \sigma(t)}{dt^{-q}} + \sigma(t) - \sigma_0 \\ = (G_m + G_e + G_\infty)(\epsilon(t) - \epsilon_0) + G_e \tau_0^{-\mu} \frac{dt^{-\mu} \epsilon(t)}{dt^{-\mu}} \\ + G_\infty \tau_0^{-q} \frac{d^{-q} \epsilon(t)}{dt^{-q}}. \end{aligned} \quad (5)$$

This model is called fractional solid model. It reduces to the fractional Zener model above Eq. (4) for $G_\infty \rightarrow 0$. For $q, \mu \rightarrow 1$ one recovers a normal Zener model with an equilibrium modulus given by $\tilde{G}_e \equiv G_e + G_\infty$.

Several experimentally relevant functions (relaxation and retardation function, complex modulus and compliance, relaxation and retardation time spectrum etc.) may be calculated via the Laplace–Mellin transform technique and can be expressed in closed form by use of Fox’s H -function.^{3,5,8,14}

Here we are interested in describing a stress-strain experiment with a harmonic external force. Hence we need the complex modulus which is given via³

$$G^*(\omega) = \frac{(G_m + G_e) + G_e (i\omega\tau_0)^{-\mu}}{1 + (i\omega\tau_0)^{-q}} + G_\infty \quad (6)$$

for the non-transient regime. The storage modulus thus becomes

$$G'(\omega) = \frac{G_{me} \tilde{\omega}^q \cos \frac{\pi q}{2} + G_e \tilde{\omega}^{q-\mu} \cos \frac{\pi(q-\mu)}{2} + G_{me} \tilde{\omega}^{2q} + G_e \tilde{\omega}^{2q-\mu} \cos \frac{\pi\mu}{2}}{\tilde{\omega}^{2q} + 2\tilde{\omega}^q \cos \frac{\pi q}{2} + 1} + G_\infty \quad (7)$$

and the loss modulus is

$$G''(\omega) = \frac{G_{me} \tilde{\omega}^q \sin \frac{\pi q}{2} + G_e \tilde{\omega}^{q-\mu} \sin \frac{\pi(q-\mu)}{2} - G_e \tilde{\omega}^{2q-\mu} \sin \frac{\pi\mu}{2}}{\tilde{\omega}^{2q} + 2\tilde{\omega}^q \cos \frac{\pi q}{2} + 1}, \quad (8)$$

where the abbreviations $\tilde{\omega} = \omega\tau_0$ and $G_{me} = G_m + G_e$ were introduced.

The relaxation time spectrum¹⁵ is given by³

$$H(\tau) = \frac{1}{\pi} \frac{G_{me} (\tau/\tau_0)^q \sin \pi q - G_e (\tau/\tau_0)^\mu \sin \pi\mu + G_e (\tau/\tau_0)^{\mu+q} \sin \pi(q-\mu)}{(\tau/\tau_0)^{2q} + 2(\tau/\tau_0)^q \cos \pi q + 1} \quad (9)$$

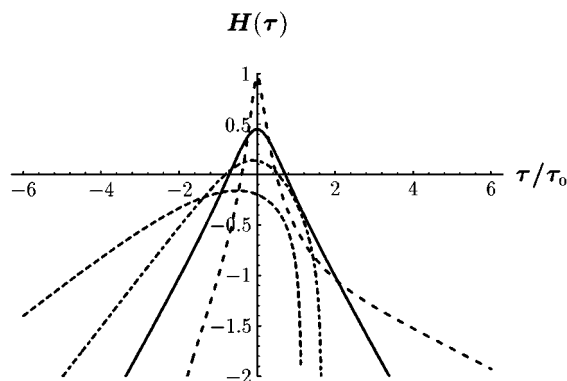


FIG. 2. Spectrum $H(\tau)$ for $G_m=9$, $G_e=1$, and the fractional parameters $q=0.3, 0.5, 0.7, 0.9$ (from left top to bottom) and $\mu=0.7$. The full line corresponds to $q=\mu$.

and shows a power law tail $H(\tau) \sim (\tau/\tau_0)^{\mu-q}$ for $\tau/\tau_0 \gg 1$. Clearly, for $\mu \rightarrow q$ the turnover point to the final long tail power law is shifted towards $\tau_{\text{top}} \rightarrow \infty$. The spectrum is displayed for various values of the fractional parameters in Figs. 2 and 3. Fig. 4 shows the change of the spectrum for simultaneously decreased q and μ with the additionally decreasing difference of both. The “hill” flattens and the shift of the turnover point is obvious. This mirrors the actual situation in the experiments discussed here.

III. FILLED POLYMERS

Since the discovery of vulcanization of natural rubber by Charles Goodyear in 1839 and the patent for the first pneu by the Belfast veterinary John Boyd Dunlop in 1888 one has been interested in improving the mechanical properties of rubber, not at least for safety and economy in automobilism.

The mechanical properties of polymer networks are massively influenced by the addition of certain filling substances (fillers).¹⁵ Whereas the quasistatic behavior of filled networks is fairly well understood¹⁶ it is the dynamics that still lacks adequate descriptions. Here, we introduced our fractional model which provides a pretty good description of

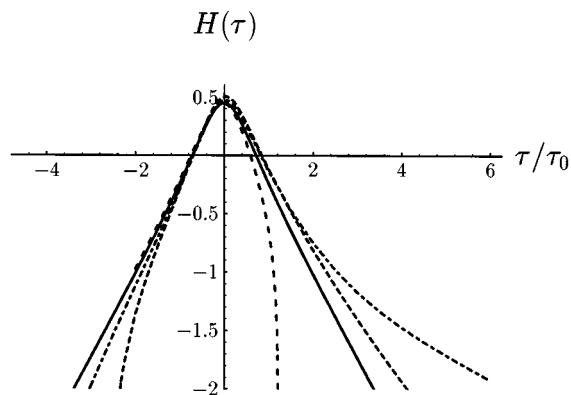


FIG. 3. Spectrum $H(\tau)$ for $G_m=9$, $G_e=1$, and the fractional parameters $q=0.7$ and $\mu=0.3, 0.5, 0.7, 0.9$ (from right top to bottom). The full line corresponds to $q=\mu$.

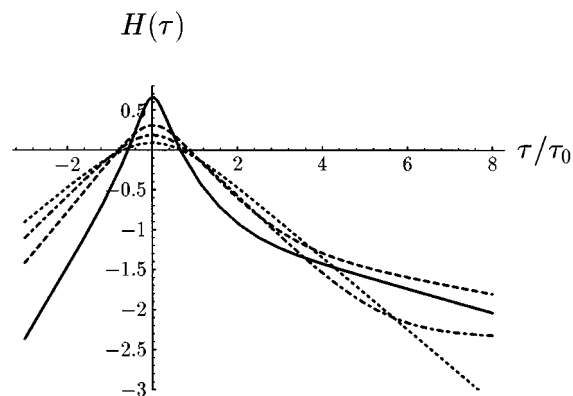


FIG. 4. Spectrum $H(\tau)$ for $G_m=9$, $G_e=1$ and the fractional parameters $q=0.8, \mu=0.65$ (—), $q=0.6, \mu=0.5$ (- - -), $q=0.52, \mu=0.515$ (- · - ·), and $q=\mu=0.45$ (····).

unfilled polymers and want to investigate its usefulness if applied to filled systems. We will show that it is also working well there and thus serves as a phenomenological description of the dynamics involved.

The increased strain energy of filled networks bases on two main issues: On the one hand adhesional contacts between polymer chains and filler surface create additional crosslinks and thus enlarge the elastic moduli. On the other hand the accessible volume of the polymer matrix is reduced by the space occupied by the filler leading to a higher intrinsic stress in the network.^{15,16} In that course the involved parameters should also vary with changing filler content, and, reversely—if experimentally measured—should retain certain information on the filler content itself.

The dynamics in complex systems are discussed parallelly to the glass forming process in Ref. 17.

IV. RESULTS

Four different series of specimens were measured by Schick,¹⁸ two apiece filled with carbon black and silicates, respectively. Here we concentrate on the silica filled series labeled NR32237 and the carbon black filled series S10 in-

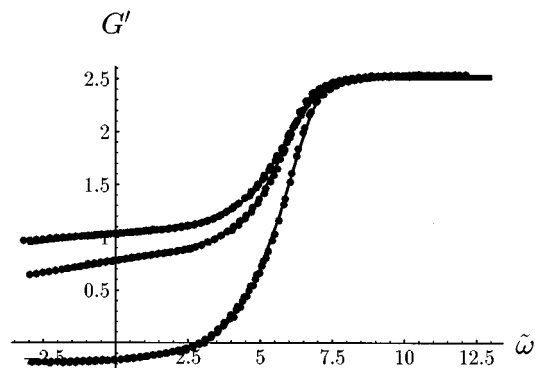


FIG. 5. Storage modulus for NR32237 with a varying filler content $F=0, 20, 40\%$ phr (from bottom to top curve).

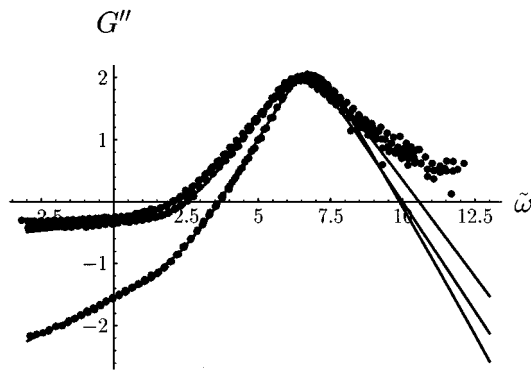


FIG. 6. Loss modulus for NR32237 with a varying filler content $F=0,20,40\%$ phr (from bottom to top curve).

volving seven and four different filler degrees respectively. The experimental measurement is seriously sensitive to preparation and handling. Thus some of the data points—especially of the two series not considered here—had to be discarded. Nevertheless there remain enough for a meaningful discussion. Filler content was varied from 0 up to 60 phr (chemical mass concentration) meaning relative mass fractions in the range 0...37.5%. Via harmonic stress-strain experiments the complex modulus was measured. By construction of a master curve one obtains the modulus in a frequency window from approximately $10^{-2.5}$ to 10^{12} c/sec.

Data fits are done by use of the standard simplex algorithm¹⁹ simultaneously executed for G' and G'' . Typical fits of the loss and storage moduli according to Eqs. (7) and (8) for three different filler contents are displayed in Figs. 5 and 6. The relaxation time spectra of the series corresponding to these figures are displayed in Fig. 7. In principle, there is similar behavior for silicate and carbon black filled networks, only the absolute magnitude of some of the characteristic quantities is different (see below). As can be seen G' is correctly described over a range of 15 decades in time whereas G'' can simultaneously be fitted over about 10 decades, only, indicating that there are additional processes not accounted

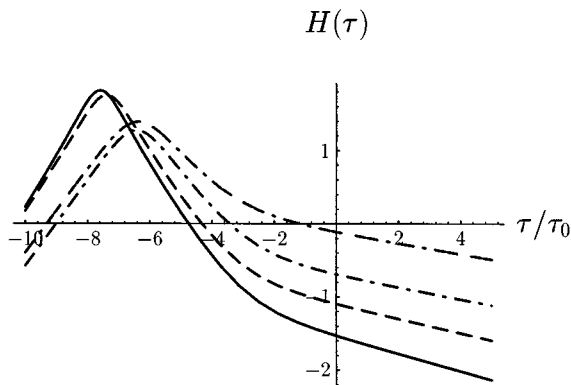


FIG. 7. Relaxation time spectrum for NR32237. Filler content: 0,30,60% phr. The higher the filler content the more the power law tail is shifted to higher vertical values.

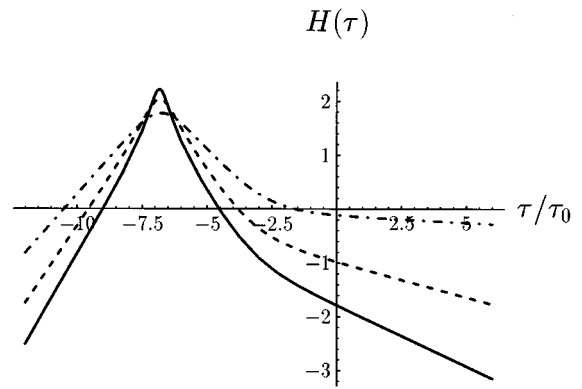


FIG. 8. Relaxation time spectrum for S10. Filler content: 0,20,40,60% phr. The higher the filler content the more the power law tail is shifted to higher vertical values.

for by our model considerably effect the dissipation. In Fig. 8 the spectra for a carbon black filled series, S10, are plotted, for comparison. Clearly, for increased filler content the maxima of the spectra are slightly shifted to higher time constants and—the major effect indeed—the center hill is flattened and the slope of the long tail is decreased showing the more and more enhanced relative existence of slower relaxation processes. This means that added filler particles causing a successively higher degree of structural inhomogeneity broaden the spectrum significantly. The range over which $H(\tau)$ is plotted is optimistically chosen to be wider than the correctly described range of the master curves in order to make the changes utterly visible.

A. Equilibrium modulus

Figure 9 shows the equilibrium modulus G_e for all specimens (except altogether 3 discarded data points). Each series of G_e is normalized in respect to its own zero value $G_e(F=0)$ where F denotes the filler content in the chemical mass fraction phr. Note that some points may represent more than one specimen. All normalized data show satisfying data collapsing indicating the independence of the actually underlying specimen's matrix. Thus having at hand these data on G_e it is not possible to distinguish between silica and carbon black filled systems. That a difference of the fit parameter

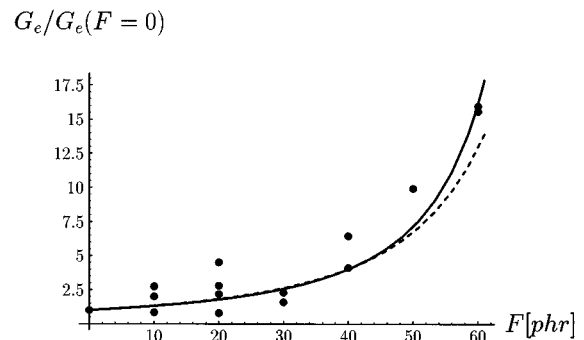


FIG. 9. Normalized equilibrium modulus vs filler content.

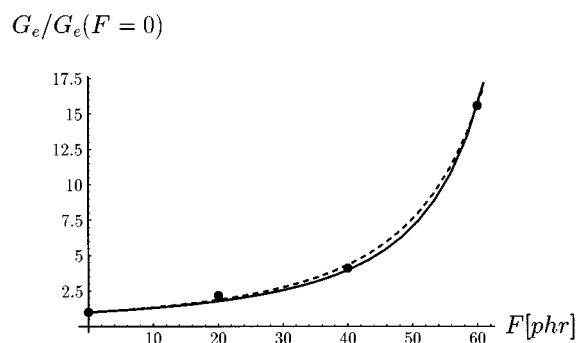


FIG. 10. Normalized equilibrium modulus vs filler content for the series S10.

F_{crit} of about 10 phr does not affect the fit's quality significantly is due to the nonlinear connection to v_{crit} (see below) that is not too much affected in this special range of variation. Fig. 10 shows the same for the series S10, exclusively (as it occurs to be the best measured of the four series).

Two models are employed to fit these data: Brinkman's formula²⁰

$$\frac{G_e}{G_0} = \left(1 - \frac{F}{F_{\text{crit}}}\right)^{-2.5}, \quad (10)$$

and Eilers' and van Dijck's formula^{21,22}

$$\frac{G_e}{G_0} = \left(1 + 1.25 \frac{F}{1 - F/F_{\text{crit}}}\right)^2, \quad (11)$$

where $G_0 \equiv G(F=0)$ is the modulus of the unfilled specimen of the actual series, and F_{crit} is a free fit parameter. For the few data points one cannot distinct upon the use of either function. Also for S10 which shows the most accurate dependence both formulas do their job well. The critical filler content is listed in Table I where for v_{crit} the critical volume fraction of the filler an à-peu-près conversion factor was applied.

Now both of these formulas show some common and very appealing features. For low values of F (and $F_{\text{crit}}=1$ for Brinkman's) they reduce to the theoretically predicted Einstein–Smallwood relation^{23,24}

$$\frac{G_e}{G_0} = 1 + 1.25 \frac{F}{100} \quad (12)$$

valid for ideal balls in suspension. For the influence of the particle shape see Ref. 16. Both formulas show a pole for $F = F_{\text{crit}}$ of about 0.8...0.9 corresponding to a volume per-

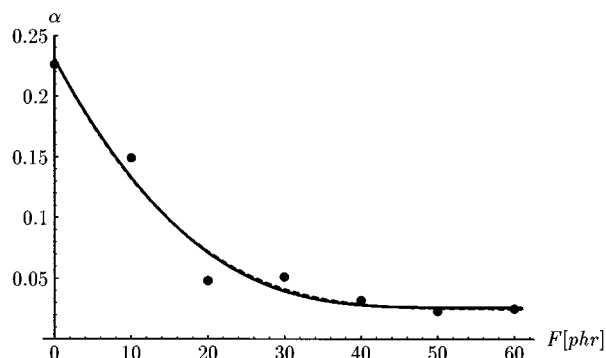


FIG. 11. Difference of the fractal parameters $\alpha = q - \mu$ for the series NR32237 fitted by modified VTF law for $F_{\text{crit}} = 0.936$ phr and 0.798 phr (dashed).

centage near 30%. These poles may be assigned critical point exponents²⁵ of $\beta = -2.5$ or -2 for Brinkman's and Eilers and van Dijck's formulas, respectively. This observation enables one to speak of critical filler concentrations in the percolation scheme: given a certain amount of filler worked into the polymer sample it will form clusters. Near the critical concentration F_{crit} the largest cluster expands in a power law divergence, the filler percolates. This causes the existence of a critical point in the dependence of G_e on F . A comparison with the percolation threshold for a three-dimensional simple cubic lattice of about 31% shows a reasonable agreement. For further discussion see Ref. 16. The formation of a filler cluster running through the whole specimen massively stiffens the sample and causes a flattened relaxation time spectrum.

Concluding this subsection it is worth remarking that by the relatively clear dependence of G_e on F —if samples are carefully handled—our model parameter G_e may be well bequested to render information on F if compared to G_0 .

B. "Homogeneity" $\alpha = q - \mu$

Besides the modulus, one is interested in the relaxation time spectrum, especially the power law regions. In spite of the data collapsing for G_e indicating a general physical mechanism of fillers upon the equilibrium modulus, α is strongly dependent on the very single series, i.e. the underlying network. α is very sensitive on the accuracy of the constructed master curves. For the NR32237 series the data points show the clear behavior plotted in Fig. 11. Fig. 12 displays the data for the carbon black filled series S10. For the silica filled samples the variation is much more significant than for the carbon black series. The last could in fact also be fitted by an exponential. Nevertheless all data points displayed in Fig. 11 are side-checked to be reliable and, in addition, both kinds of fillers should cause a similar effect. Formula (13) is thus applied to both of them showing nice agreement (even for Fig. 12 this is a meaningful statement despite of the use of three fit parameters to merely four data points as Eq. (13) issues a very unique behavior). For $F=0$ α bears its largest value (maximum presence of polymer). Addition of filler causes a decreasing of α and for $F \rightarrow F_{\text{crit}}$

TABLE I. Critical parameters for the equilibrium modulus.

Formula	Series	F_{crit}	v_{crit}
Eilers and van Dijck	all	0.798	0.28
	S10	0.805	0.29
Brinkman	all	0.936	0.32
	S10	0.901	0.31

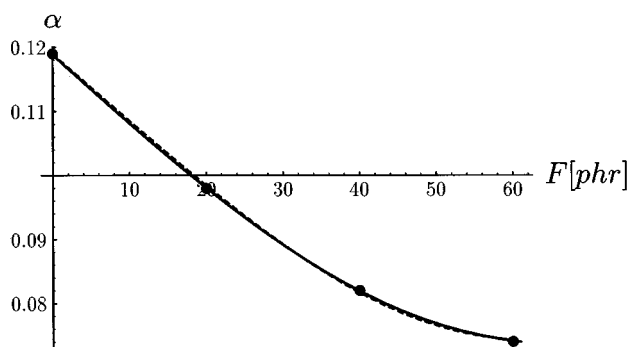


FIG. 12. Difference of the fractal parameters $\alpha = q - \mu$ for the series S10. Fit by modified VTF law for $F_{\text{crit}} = 0.901$ phr and 0.805 phr (dashed).

only a small constant value responsible for the polymer occupying the remaining space in between the percolating filler should be left whereas the filler's contribution vanishes identical to zero. A possible function fulfilling these requirements is the modified Vogel–Tamann–Fulcher (VTF) relation:

$$\alpha = \alpha_{\text{rem}} + \alpha_{\text{var}} = \alpha_{\text{rem}} + \alpha_0 \exp \frac{\beta}{F - F_{\text{crit}}}, \quad (13)$$

where α_{rem} denotes the remaining polymer for the critically filled system and varying α_{var} is caused by polymer successively replaced by filler material. Equation (13) has a horizontal asymptote issuing the critical behavior in the vicinity of F_{crit} . The value of the critical filler concentration is taken from the G_e fit.

α_0 is about 0.025 for NR32237 and 0.074 for S10. Thus α_0 may be a candidate parameter to distinguish between filler types. Of course this statement needs verification by further experimental results not accessible to us so far.

This way, for the description of both quantities, equilibrium modulus and α altogether 4 fit parameters are needed. α may be interpreted as a measure of homogeneity. For successively added filler, i.e. for increasing structural inhomogeneity, α is decreasing. Both G_e and α show clear behaviors in their variance upon F and vary in an expected manner.

C. Other parameters

The behavior of all the involved fit parameters for S10 is shown in Table II. Concerning the other occurring parameters not discussed so far. G_m stays approximately constant within one series but is dependent on the underlying network, i.e. dependent on the single series. Thus it is a charac-

TABLE II. Parameters of the fractional model for the series S10.

Filler content [phr]	q	μ	G_m	G_e	G_{inf}	τ_0
0	0.663	0.544	253	2.10	0.547	$2.60 \cdot 10^{-8}$
20	0.631	0.535	254	4.82	0.713	$4.27 \cdot 10^{-8}$
40	0.556	0.474	246	21.0	0	$3.33 \cdot 10^{-7}$
60	0.551	0.477	217	53.1	0	$4.54 \cdot 10^{-7}$

teristic quantity of the free network exclusively. Both of the single fractional parameters, q and μ , decay with increasing filler content and q ranges in between ca. 0.8...0.5. The fractal parameters influence the whole shape of the modulus over the frequency axis so that both underlying network and filler are responsible for their actual quantities. The range over which q ranges for silica filled samples is approximately of a factor of 2 in comparison to both of the carbon black series. It is thus a reliable differentiation upon the filler type if a whole series on $F = 0, \dots, F \approx F_{\text{crit}}$ is available. G_{∞} is always relatively small—mostly even less than one—so that it is only relevant for small filler concentrations where it is about a factor of 4 less than G_e . It determines the slope of the storage modulus for low frequencies. τ_0 is merely a horizontal shift in the log–log plot. It does vary within one order of magnitude. As G_m is à-peu-près constant η_m is varied inversely proportional to τ_0 .

V. CONCLUSIONS

The concept of fractional relaxation was successfully applied to describing filled polymer networks. Despite the growing structural inhomogeneity with the addition of filler material this homogeneous phenomenological concept does provide an appropriate tool to modeling relaxation dynamics.

The equilibrium modulus shows a critical behavior in consistence with a simple percolation picture. The functional form follows well-known relations developed by Eilers and van Dijk and Brinkman. In this scheme of percolation the filler constitutes clusters the correlation length of which diverges in the vicinity of F_{crit} . By the same time the relaxation time spectrum becomes more and more flat involving a relatively higher percentage of longer relaxation times. The dependence of $\alpha = q - \mu$ on F may be described by a Vogel–Tamann–Fulcher law with an additional constant.

A clear dependence on F is exhibited by both G_e and α but they do not give knowledge about the type of the filler particles. This is provided by the range of variance of the fractional parameter q being of a factor of about 2 for silica particles in comparison to carbon black.

ACKNOWLEDGMENTS

The first author wants to thank W. G. Glöckle for fruitful and instigating discussions. This paper was supported by the Deutsche Forschungsgemeinschaft (SFB 239, projects C7 and C8).

¹M. Ghosh and B. K. Chakrabarti, *Ind. J. Phys.* **65A**, 1 (1991).

²T. V. Ramakrishnan and M. Raj Lakshmi, *Non-Debye Relaxation in Condensed Matter* (World Scientific, Singapore, 1987).

³W. G. Glöckle and T. F. Nonnenmacher, *Macromolecules* **24**, 6426 (1991).

⁴W. G. Glöckle, thesis, University of Ulm, 1993.

⁵W. G. Glöckle and T. F. Nonnenmacher, *J. Stat. Phys.* **71**, 741 (1993).

⁶W. G. Glöckle and T. F. Nonnenmacher, in *Fractals in Biology and Medicine*, edited by T. F. Nonnenmacher, G. A. Losa, and E. R. Weibel (Birkhäuser, Basel, 1993).

⁷W. G. Glöckle and T. F. Nonnenmacher, *Rheol. Acta* **33**, 337 (1994).

⁸T. F. Nonnenmacher and W. G. Glöckle, *Philos. Mag. Lett.* **64**, 89 (1991).

⁹T. F. Nonnenmacher, in *Rheological Modeling: Thermodynamical and Statistical Approaches*, Vol. 381 in Lecture Notes in Physics, edited by J. Casas-Vázquez and D. Jou (Springer, Berlin, 1991), pp. 309–320.

- ¹⁰C. Friedrich and H. Braun, *Rheol. Acta* **31**, 309 (1992).
- ¹¹N. W. Tschoegl, *The Phenomenological Theory of Linear Viscoelastic Behavior* (Springer, Berlin, 1989).
- ¹²H. Schiessel and A. Blumen, *J. Phys. A.* **26**, 5057 (1993).
- ¹³N. Heymans and J.-C. Bauwens, *Rheol. Acta* **33**, 210 (1994).
- ¹⁴A. M. Mathai and R. K. Saxena, *The H-Function with Applications in Statistics* (Wiley, New Delhi, 1978).
- ¹⁵J. D. Ferry, *Viscoelastic Properties of Polymers* (Wiley, New York, 1970).
- ¹⁶H. G. Kilian, M. Strauss, and W. Hamm, *Rubber Chem. Technol.* **67**, 1 (1994).
- ¹⁷N. G. McCrum, B. E. Read, and G. Williams, *Anelastic and Dielectric Effects in Polymer Solids* (Wiley, London, 1967).
- ¹⁸W. Schick, diploma thesis, University of Ulm, 1992.
- ¹⁹J. A. Nelder and R. Mead, *Comput. J.* **7**, 308 (1965).
- ²⁰H. C. Brinkman, *J. Chem. Phys.* **20**, 571 (1952).
- ²¹H. Eilers, *Kolloid-Z.* **97**, 313 (1941).
- ²²C. van der Poel, *Rheol. Acta* **1**, 198 (1958).
- ²³A. Einstein, *Ann. Phys. IV* **19**, 289 (1906); *Kolloid-Z* **27**, 137 (1920).
- ²⁴H. M. Smallwood, *J. Appl. Phys.* **15**, 758 (1944).
- ²⁵H. G. Stanley, *Introduction to Phase Transitions and Critical Phenomena* (Clarendon, Oxford, 1971).